

Role of goethite during air-oxidation of PAH-contaminated soils

Coralie Biache, Olivier Kouadio, Khalil Hanna, Catherine Lorgeoux, Pierre
Faure

► **To cite this version:**

Coralie Biache, Olivier Kouadio, Khalil Hanna, Catherine Lorgeoux, Pierre Faure. Role of goethite during air-oxidation of PAH-contaminated soils. *Chemosphere*, Elsevier, 2014, 117, pp.823-829. 10.1016/j.chemosphere.2014.11.004 . hal-01101620

HAL Id: hal-01101620

<https://hal-univ-rennes1.archives-ouvertes.fr/hal-01101620>

Submitted on 13 Jan 2015

HAL is a multi-disciplinary open access archive for the deposit and dissemination of scientific research documents, whether they are published or not. The documents may come from teaching and research institutions in France or abroad, or from public or private research centers.

L'archive ouverte pluridisciplinaire **HAL**, est destinée au dépôt et à la diffusion de documents scientifiques de niveau recherche, publiés ou non, émanant des établissements d'enseignement et de recherche français ou étrangers, des laboratoires publics ou privés.

Role of goethite during air-oxidation of PAH-contaminated soils

Coralie Biache^{1,2,*}, Olivier Kouadio^{1,2}, Khalil Hanna³, Catherine Lorgeoux^{4,5}, Pierre Faure^{1,2}

¹ Université de Lorraine, LIEC, UMR7360, Vandœuvre-lès-Nancy, F-54506, France

² CNRS, LIEC, UMR7360, Vandœuvre-lès-Nancy, F-54506, France

³ École Nationale Supérieure de Chimie de Rennes, UMR CNRS 6226, 11 Allée de Beaulieu, F-35708 Rennes Cedex 7, France.

⁴ Université de Lorraine, GeoRessources, UMR7359, Vandœuvre-lès-Nancy, F-54506, France

⁵ CNRS, GeoRessources, UMR7359, Vandœuvre-lès-Nancy, F-54506, France

* Corresponding author

Address: LIEC, Faculté des Sciences et Techniques

Boulevard des Aiguillettes

B.P. 70239

54506 Vandoeuvre-lès-Nancy Cedex

France

E-mail: coralie.biache@yahoo.fr (C. Biache)

Phone: (+33) 3 83 68 47 40

24 **Abstract**

25 The impact of goethite on air-oxidation of PAH-contaminated soils was studied through two
26 sets of experiments. (i) Soil extractable organic matter (EOM) and (ii) whole coking plant
27 soils were oxidized at 60 and 100 °C for 160 days, with/without goethite. Organic matter
28 (OM) mineralization was monitored via CO₂ production and polycyclic aromatic compounds
29 (PACs) oxidation was investigated by GC-MS analyses. The decrease in EOM and PAH
30 contents, and the oxygenated-PAC production observed during EOM oxidation, were
31 enhanced by the presence of goethite. PACs were likely transformed at the goethite surface
32 through electron transfer process. Mass carbon balance revealed a transfer from EOM to the
33 insoluble organic fraction indicating condensation/polymerization of organics. Soil oxidation
34 induced a decrease in EOM, PAH but also in oxygenated-PAC contents, underscoring
35 different oxidation or polymerization behavior in soil. The goethite addition had a lesser
36 impact suggesting that indigenous minerals played an important role in PAC oxidation.

37 **Keywords:** contaminated soil; polycyclic aromatic compound (PAC); oxygenated-PAC;
38 goethite; oxidation

39

40 1. Introduction

41

42 Iron oxides are the most abundant metallic oxides in soils (Schwertmann and Taylor, 1989),
43 they are present in most soils and encompass oxides, oxyhydroxides and hydrated oxides. Fe-
44 minerals are known to play an active part in the organic contamination fate as they represent
45 strong sorption surfaces for pollutants and they catalyze many important redox
46 transformations (Borch et al., 2009). During the past decades their ability to participate in
47 such redox reactions was involved in remediation strategies for organic contamination. For
48 instance Fe-minerals are associated with H_2O_2 to produce hydroxyl radicals that can degrade
49 organic compounds in Fenton-like reactions. Soil iron minerals i.e. magnetite, hematite,
50 goethite, and ferrihydrite, are all able to catalyze H_2O_2 (Yap et al., 2011).

51 Fenton-like reaction has been investigated for the remediation of water and soil contaminated
52 with halogenated solvent, pesticides and petroleum hydrocarbons (Watts and Stanton, 1999;
53 Usman et al., 2013). Fenton-like reaction shows also a great potential for polycyclic aromatic
54 hydrocarbon (PAH, compounds constituted of two, or more, fused benzene rings) degradation
55 in contaminated soils (Nam et al., 2001; Usman et al., 2012). The catalytic role of iron oxides
56 for Fenton-like reaction is extensively studied for chemical remediation purpose. However
57 such treatments are not automatically applied to contaminated soils and little is known about
58 the involvement of iron oxide in processes occurring during natural attenuation of
59 contaminated soils, especially abiotic oxidation. Some authors studied iron oxide-mediated
60 oxidative transformations of organic compounds (Zhang and Huang, 2007; Lin et al., 2012)
61 but the experiments were designed with solids suspended in aqueous solution which is not
62 representative of real soil conditions. Wang et al. (2009) studied pyrene degradation on iron
63 oxide under UV radiation and evidenced photocatalytic effect of several iron oxide. In real

64 soils UV light affects only the surface layers since its intensity decays rapidly in the solid
65 phase. Abiotic oxidation still occurs in deeper layer but so far this process was scarcely
66 investigated, probably due to the difficulty to study this process independently to others. This
67 difficulty can be bypassed using experimental simulation. Indeed low-temperature oxidations
68 (60-130 °C) are proven to successfully mimic long-term abiotic oxidation of fossil organic
69 matter (OM) (Faure et al., 1999; Elie et al., 2000; Blanchart et al., 2012). Such experiments
70 were extensively used in the 1980s to study coal weathering and its impact on coal heating
71 properties (Gethner, 1987; Calemma et al., 1988; Jakab et al., 1988). More recently, low-
72 temperature oxidations of PAH-contaminated matrices showed that minerals (e.g. clay
73 minerals and calcite) play an important role on the contamination fate (Ghislain et al., 2010;
74 Biache et al., 2011; Biache et al., 2014). Indeed, oxidation causes a production of oxygenated-
75 polycyclic aromatic compounds (O-PACs: PAH with oxygenated moieties e.g. alcohol,
76 ketone, aldehyde groups) and formation of an insoluble carbonaceous residue, supposedly
77 through oxidative polymerization, leading to the contamination stabilization. PAH-
78 contaminated soils often contain high proportion of iron oxide and other metal oxides (Biache
79 et al., 2014), however their influence on PAC oxidation has never been investigated in such
80 context.

81 Therefore, this study reported a first investigation on the role of iron oxide (goethite) on
82 PAC fate (including PAHs and O-PACs) during abiotic air-oxidation of contaminated soils.
83 Its aim was to determine which mechanisms were involved during this major process involved
84 in natural attenuation. Goethite (α -FeOOH) was selected because it is one of the most
85 thermodynamically stable and the most abundant iron (oxy)(hydr)oxide in natural
86 environments (Schwertmann and Cornell, 2007).
87 Two sets of experiments were performed. The first one was conducted on extractable organic
88 matter (EOM) previously isolated from PAC-contaminated soils. Afterwards, EOM was

89 mixed with goethite or silica sand; the latter was used as inert support since its reactivity
90 towards organic compounds is limited (Ghislain et al. 2010). The second experiment was
91 performed directly on soils, raw or supplemented with goethite. These two sets allowed
92 investigating two levels of increasing complexity by studying the influence of an iron oxide
93 on the soil EOM, which could give more precise information on the involved mechanisms,
94 and on the whole soil including indigenous minerals, which is more complex but also more
95 realistic. Oxidations were performed at 60 and 100 °C, the latter allowing more advanced
96 oxidation and the first one representing an intermediate between 100 °C and field
97 temperatures.

98

99 **2. Materials and Methods**

100 2.1. Samples

101 Soils were sampled at two former coking plant sites (Homécourt and Neuves-Maisons,
102 France), then freeze-dried, sieved (2 mm) and crushed (500 µm). EOM was recovered by
103 extracting parts of the soils in Soxhlet apparatus (CHCl₃, 24 h), it contains PACs and other
104 organics of various size, from macromolecules (asphaltenes) to mono-aromatic units. Neuves-
105 Maisons and Homécourt EOMs were concentrated at 1.4 and 2.4 mg/mL, respectively. Soils
106 were also used directly or mixed with goethite.

107

108 2.2. Minerals

109 The silica sand was Fontainebleau sand (180-500 µm, Carlo Erba) used as a non-reactive
110 reference in the EOM experiment.

111 Goethite (α -FeOOH) was synthesized according to Schwertmann and Cornell (2007).
112 Briefly, sample was prepared by air-oxidation of a hydrolyzed FeSO₄ solution according to
113 Prélot et al. (2003) (cf. supporting information).

114 Minerals were washed with dichloromethane prior experiments to prevent organic
115 contamination.

116

117 2.3. Oxidation experiment

118 EOMs and soils were mixed with minerals according to the following proportions: silica
119 sand (2 g) and goethite (0.5 g) mixed with Homécourt (47.1 mg) and Neuves-Maisons (48.7
120 mg) EOMs, Homécourt (2.5 g) and Neuves-Maisons (5 g) soils taken alone or mixed with
121 goethite (0.5 g) (Table S1). Soils and minerals were placed in 100 mL glass bottles equipped
122 with open caps and PTFE/silicone septa. EOM aliquots were added to the minerals to reach
123 the mineral/EOM proportions specified in Table S1. Bottles were left open in a ventilated
124 hood until complete evaporation of the solvent.

125 Two sample sets were prepared and placed in ovens at 60 and 100 °C. CO₂ released in the
126 bottles was measured weekly by an infrared absorbance measurement ($\lambda = 2325.6 \text{ cm}^{-1}$) with
127 an infrared Binos analyzer. The measured CO₂ was normalized to the initial sample total
128 organic carbon (TOC) content. After each measurement bottles were opened to renew the
129 atmosphere and the septa were replaced. After 160 days, samples were removed from the
130 ovens and, after CO₂ measurements, were stored at -18 °C prior analyses.

131

132 2.4. Extraction

133 Samples were transferred to 250 mL boiling flasks and chloroform (100 mL) was added to
134 each flask. The mixtures were heated at 60 °C and stirred for 45 min before being filtered on
135 GF/F Whatman glass-fiber filters. The filtrates were concentrated under a gentle nitrogen flow
136 and volumes were adjusted to 20 mL. For each sample, an EOM fraction (3 mL) was
137 transferred to a pre-weighed bottle and the EOM content was determined after solvent
138 evaporation.

139

140 2.5. PAC quantification

141 An internal PAH standard mix of [²H₈]naphthalene, [²H₁₀]acenaphthene,
142 [²H₁₀]phenanthrene, [²H₁₂]chrysene, [²H₁₂]perylene (25 µL at 16 µg/mL, Cluzeau) was added
143 to the EOM (75 µL) before being injected in a gas chromatograph coupled with a mass
144 spectrometer (GC-MS). The GC-MS was previously internally calibrated with the internal
145 standards listed above for 16 PAHs plus 4 O-PACs (Table 1) at 6 concentrations (0.5, 1, 2, 4,
146 6 and 8 µg/mL). The GC was a Shimadzu GC-2010 Plus, equipped with a silica-glass
147 capillary column DB-5MS (60 m × 0.25 mm i.d. × 0.1 µm film thickness) coupled with a
148 QP2010-Ultra (Shimadzu) MS in fullscan mode with a transfer line heated at 300 °C. The
149 oven temperature program was as follow: 70 °C for 2 min, from 70 to 130 °C at 15 °C/min,
150 then from 130 to 315 °C at 3 °C/min and then a 15-min hold at 315 °C. Helium was used as
151 carrier gas in constant flow mode (1.4 mL/min).

152

153 2.6. TOC content

154 TOC contents were determined in soils and EOM/mineral mixtures with a total carbon
155 analyser TOC-V CSH (Shimadzu) associated with a solid sample module SSM-5000A
156 (Shimadzu).

157

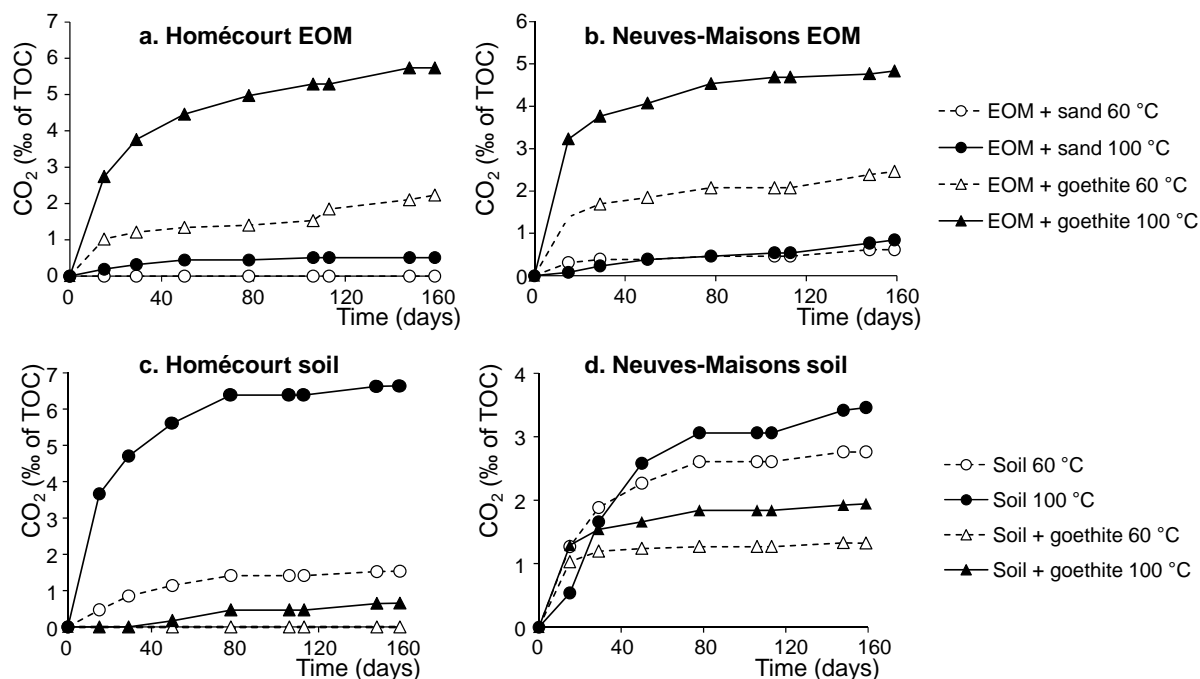
158 3. Results

159 3.1. EOM/minerals mixture

160 3.1.1. CO₂ production

161 For both samples, CO₂ production of the EOM/mineral mixture followed the same trend
162 (Figure 1a,b). The maximum production was observed for the EOM/goethite mixtures

163 oxidized at 100 °C and reached about 6 and 5‰ of TOC for Homécourt and Neuves-Maisons,
 164 respectively. It was followed by the CO₂ produced by the EOM/goethite mixture during the
 165 60 °C oxidation. Smaller amount of CO₂ were observed for the EOM/sand mixture
 166 oxidations.

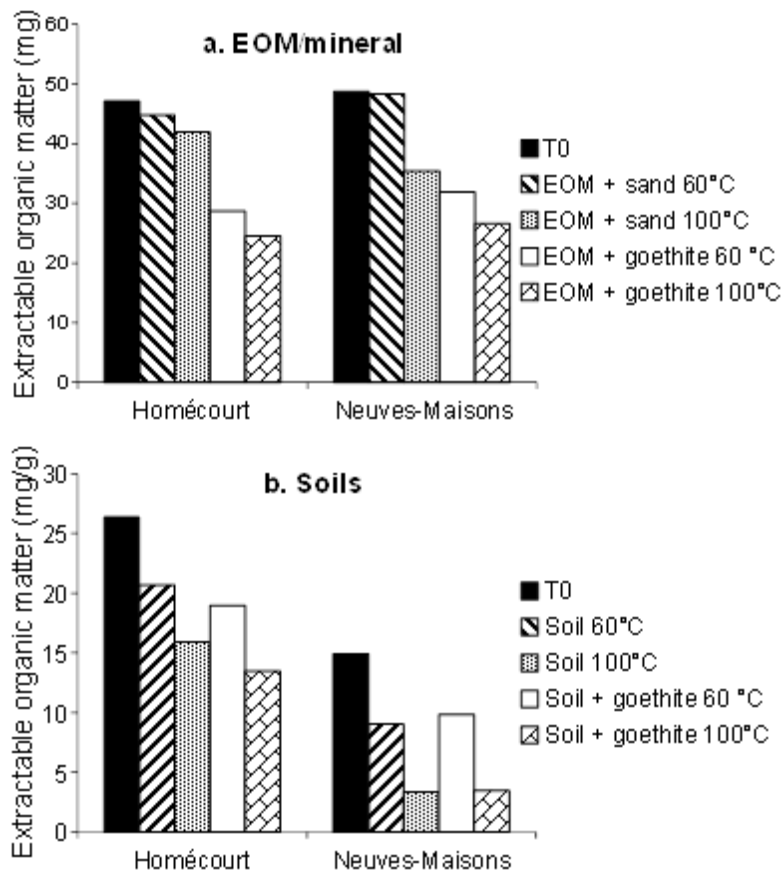


167
 168 *Figure 1: CO₂ production during the 60 and 100 °C oxidation experiments of the extractable organic*
 169 *matter (EOM) from (a.) Homécourt and (b.) Neuves-Maisons samples, mixed with silica sand and*
 170 *goethite, and (c.) Homécourt and (d.) Neuves-Maisons soils and soils mixed with goethite.*

171

172 3.1.2. EOM contents

173 Overall, oxidations induced a decrease in the EOM content of the EOM/mineral mixtures
 174 (Figure 2a). It was limited for the EOM/sand mixtures oxidized at 60 °C and was more
 175 important for the same mixture oxidized at 100 °C but clearly lower than the EOM/goethite
 176 mixtures. The decrease was similar for both Homécourt and Neuves-Maisons samples at 100
 177 °C and went from 47.1 to 24.5 mg and from 48.7 to 26.6 mg, respectively.



178

179 *Figure 2: Extractable organic matter (EOM) contents after the 60 and the 100 °C oxidation*
 180 *experiment of (a.) Homécourt and Neuves-Maisons EOM/mineral mixtures, and (b.) Homécourt and*
 181 *Neuves-Maisons soil and soil/goethite mixtures.*

182

183 3.1.3. PAH contents

184 Overall, EOM/mineral mixture oxidations induced a decrease in PAH concentrations. For
 185 Homécourt EOM/sand mixture it was limited to 5% after the 60 °C experiment (Table 1). It
 186 was more important at 100 °C (49%), mostly because of the loss of low molecular weight
 187 (LMW) compounds compared to high molecular weight (HMW), as shown by the
 188 LMW/HMW ratio which went from 3.1 to 1 (Table 1). The 60 and 100 °C experiments
 189 induced a decrease in PAH content of 27% and 59% for Homécourt EOM/goethite mixture,
 190 respectively. It affected again mainly LMW PAHs, especially the 2- and 3-ring PAHs (Table
 191 1, Figure S3).

192 Contrary to the Homécourt EOM/sand mixture, PAHs decreased notably (40%; Table 1) after
193 the 60 °C oxidation of the Neuves-Maisons EOM/sand mixture. This decrease affected both
194 LMW and HMW compounds (Table 1, Figure S4). It was confirmed by the LMW/HMW ratio
195 which was barely modified (Table 1). At 100 °C, the PAH decrease was more important and
196 reached 61%. The LMW PAH, especially the 2- and 3-ring compounds were more affected
197 (Table 1, Figure S4). Neuves-Maisons EOM/goethite mixture oxidations induced also a
198 decrease in the PAH contents. It was relatively close whatever the temperature (63% at 60 °C
199 and 66% at 100 °C; Table 1)

200

201 *3.1.4. O-PAC contents*

202 Overall, oxidations induced an increase in the O-PAC contents (Table 1). For Homécourt
203 EOM, it was more important at 60 °C than at 100 °C. It was also higher when the EOM was
204 mixed with goethite than when mixed with sand (Table 1). The O-PAC production concerned
205 mostly 9-fluorenone and anthracene-9,10-dione (Table 1, Figure S5). The increase in O-PAC
206 concentrations in Neuves-Maisons EOM/mineral mixtures was higher at 100 °C than at 60 °C
207 (Table 1). The maximum O-PAC production reached 203% when Neuves-Maisons EOM was
208 mixed with goethite and oxidized at 100 °C (Table 1). This increase affected mostly
209 benzo[*de*]anthracene-7-one and benz[*a*]anthracene-7,12-dione (Table 1, Figure S6).

210 .

Table 1: PAH and O-PAC contents (in $\mu\text{g/g}$) of the initial and oxidized (60 °C and 100 °C) extractable organic matter (EOM)/mineral mixture

| $\mu\text{g/g}$ | Homécourt | | | | | Neuves-Maisons | | | | |
|---------------------------------------|-----------|------------------|-------------------|-------------------|--------------------|----------------|------------------|---------------------|-------------------|--------------------|
| | Initial | EOM/sand 60°C | EOM/sand 100°C | EOM/goet. 60°C | EOM/goet. 100°C | Initial | EOM/sand 60°C | EOM/sand 100°C C | EOM/goet. 60°C | EOM/goet. 100°C |
| Naphthalene | 17 | 2.0 | n.d. | n.d. | n.d. | 240 | 7.6 | n.d. | n.d. | n.d. |
| Acenaphthylene | 290 | 250 | 160 | 160 | 93 | 170 | 99 | 26 | 49 | 24 |
| Acenaphthene | 600 | 410 | n.d. | 61 | n.d. | 150 | 71 | n.d. | n.d. | n.d. |
| Fluorene | 410 | 260 | 20 | 39 | 22 | 120 | 65 | 2.5 | 7.0 | 1.3 |
| Phenanthrene | 750 | 760 | 150 | 720 | 320 | 390 | 270 | 21.1 | 130 | 34 |
| Anthracene | 220 | 260 | 120 | 150 | 67 | 170 | 150 | 37 | 39 | 31 |
| Fluoranthene | 400 | 550 | 300 | 560 | 260 | 550 | 440 | 220 | 320 | 220 |
| Pyrene | 290 | 320 | 240 | 310 | 200 | 450 | 290 | 180 | 200 | 150 |
| Benz[<i>a</i>]anthracene | 190 | 150 | 140 | 140 | 46 | 480 | 290 | 220 | 160 | 160 |
| Chrysene | 150 | 180 | 190 | 180 | 170 | 500 | 330 | 310 | 240 | 310 |
| Benzo[<i>b</i>]fluoranthene | 210 | 180 | 260 | 170 | 190 | 650 | 360 | 350 | 300 | 340 |
| Benzo[<i>k</i>]fluoranthene | 61 | 57 | 71 | 54 | 56 | 320 | 210 | 200 | 140 | 170 |
| Benz[<i>a</i>]pyrene | 140 | 130 | 39 | 94 | 4.9 | 500 | 290 | 110 | 150 | 0.6 |
| Indeno[<i>cd</i>]pyrene | 110 | 85 | 100 | 83 | 74 | 490 | 260 | 260 | 190 | 230 |
| Dibenz[<i>a,h</i>]anthracene | 34 | 63 | 69 | 68 | 44 | 170 | 81 | 110 | 58 | 92 |
| Benzo[<i>ghi</i>]perylene | 84 | 120 | 140 | 110 | 89 | 370 | 210 | 200 | 160 | 190 |
| Sum of PAHs | 3956 | 3777 | 1999 | 2899 | 1636 | 5720 | 3424 | 2247 | 2143 | 1953 |
| PAH decrease (%) | | 5 | 49 | 27 | 59 | | 40 | 61 | 63 | 66 |
| LMW/HMW ^a | 3.1 | 2.9 | 1.0 | 2.2 | 1.4 | 0.6 | 0.7 | 0.3 | 0.5 | 0.3 |
| 9-Fluorenone | 530 | 780 | 680 | 1500 | 1200 | 160 | 180 | 48 | 180 | 130 |
| Anthracene-9,10-dione | 140 | 240 | 190 | 420 | 450 | 110 | 110 | 47 | 120 | 97 |
| Benzo[<i>de</i>]anthracene-7-one | 5.7 | 78 | n.d. | 82 | n.d. | 130 | 350 | 530 | 240 | 550 |
| Benz[<i>a</i>]anthracene-7,12-dione | n.d. | n.d. | 120 | 71 | n.d. | 64 | 130 | 430 | 150 | 630 |
| Sum of O-PACs | 676 | 1098 | 990 | 2073 | 1650 | 464 | 770 | 1055 | 690 | 1407 |
| O-PAC production (%) | | 62 | 46 | 207 | 144 | | 66 | 127 | 52 | 203 |
| %O-PAC (/total PAC) | 15 | 23 | 33 | 42 | 50 | 8 | 18 | 32 | 24 | 42 |

212 ^aLMW/HMW = ratio of sum of naphthalene to pyrene relative to sum of benzo[*a*]anthracene to benzo[*ghi*]perylene

213 3.2. Soils and soil/goethite mixtures

214 3.2.1. CO₂ production

215 For Homécourt soil, the CO₂ production was higher when the raw soil was oxidized at 100 °C
216 and reached 7‰ of the TOC at the end of the experiment (Figure 1c). The CO₂ production
217 was much lower at 60 °C and reached less than 2‰ of the TOC. It was followed by the
218 Homécourt soil/goethite mixture oxidized at 100 °C whereas the same mixture produced
219 nearly no CO₂ at 60 °C (Figure 1c).

220 Similar pattern was observed for the Neuves-Maisons soil with a maximum CO₂ production
221 for the raw soil oxidized at 100 °C which reached about 4‰ of the TOC. However the
222 differences between the modalities were less pronounced and the minimum CO₂ production
223 observed for the Neuves-Maisons/goethite mixture oxidized at 60 °C reached 1.3‰ of the
224 TOC (Figure 1d).

225 It should be noted that a part of the generated gas could result from CO₂ desorption from soil
226 solid surfaces (e.g. minerals, OM) over the soil thermal treatments, but this process may be
227 insignificant under our experimental conditions (Sumner, 2000).

228 3.2.2. EOM contents

229 Soil oxidations led to a decrease in the EOM contents (Figure 2b). For both soils and
230 soil/goethite mixtures, it was more important at 100 °C than at 60 °C. This decrease was
231 enhanced by the presence of goethite in the case of Homécourt samples for which the EOM
232 went from 26.4 to 19.0 and to 13.5 mg/g of soil after the 60 and the 100°C experiments,
233 respectively. Surprisingly, no difference was observed with goethite addition to the Neuves-
234 Maisons soil (Figure 2b).

235 3.2.3. PAH contents

236 Oxidations induced a strong decrease in the PAH concentrations for both soils. It was more
237 important at 100 than at 60 °C and was maximum when goethite was added to the soil (92%
238 of decrease for both samples; Table 2). For both samples, the 60 °C experiments affected
239 slightly more HMW than LMW compounds, as shown by the increasing LMW/HMW ratios
240 (Table 2). On the contrary, the 100 °C experiment induced a decrease in this ratio, indicating
241 a preferential loss of the LMW PAHs (Table 2, Figures S7 and S8).

242 3.2.4. *O-PAC contents*

243 Overall, the soil and soil/goethite mixture oxidations induced a decrease in the O-PAC
244 contents. For the raw Homécourt soils, it was limited to 3% after the 100 °C experiment and
245 reached 12% after the 60 °C oxidation. This decrease was higher when Homécourt soil was
246 mixed with goethite and attained 18% and 41% after the 60 and the 100 °C experiments,
247 respectively (Table 2, Figure S9).

248 The abatement rates were higher for the Neuves-Maisons soil with 54% and 60% after the 60
249 and the 100 °C experiment on the raw soil, respectively. Goethite supplementation also
250 enhanced this decrease but the proportion of O-PAC abatement was similar for both
251 temperatures (71%; Table 2, Figure S10).

Table 2: PAH and O-PAC contents (in µg/g) of the initial and oxidized (60 °C and 100 °C) soils and soil/mineral mixtures

| µg/g | Homécourt | | | | | Neuves-Maisons | | | | |
|--------------------------------------------|-----------|--------------|---------------|--------------------|---------------------|----------------|--------------|-----------------|--------------------|---------------------|
| | Initial | Soil 60°C | Soil 100°C | Soil/goet. 60°C | Soil/goet. 100°C | Initial | Soil 60°C | Soil 100°C C | Soil/goet. 60°C | Soil/goet. 100°C |
| Naphthalene | 9.4 | 4.5 | 0.3 | 3.6 | n.d. | 74 | 26 | 3.6 | 12 | n.d. |
| Acenaphthylene | 160 | 65 | 48 | 57 | 40 | 52 | 15 | 4.0 | 13 | 4.0 |
| Acenaphthene | 340 | 18 | n.d. | 13 | n.d. | 46 | 2.0 | n.d. | 1.6 | n.d. |
| Fluorene | 230 | 26 | 13 | 22 | 9.1 | 36 | 2.4 | 0.3 | 1.9 | 0.2 |
| Phenanthrene | 420 | 240 | 140 | 200 | 14 | 120 | 47 | 19 | 28 | 6.3 |
| Anthracene | 130 | 47 | 24 | 40 | 21 | 52 | 18 | 3.3 | 10 | 2.9 |
| Fluoranthene | 220 | 120 | 68 | 120 | 15 | 170 | 94 | 33 | 73 | 17 |
| Pyrene | 160 | 73 | 26 | 61 | n.d. | 140 | 68 | 11 | 44 | n.d. |
| Benz[<i>a</i>]anthracene | 110 | 32 | 15 | 20 | 3.6 | 150 | 55 | 10 | 22 | 1.7 |
| Chrysene | 81 | 34 | 25 | 31 | 6 | 150 | 57 | 33 | 45 | 15 |
| Benzo[<i>b</i>]fluoranthene | 120 | 37 | 39 | 38 | 23 | 200 | 81 | 53 | 75 | 42 |
| Benzo[<i>k</i>]fluoranthene | 34 | 13 | 9.5 | 12 | 5.3 | 97 | 27 | 15 | 25 | 9.0 |
| Benz[<i>a</i>]pyrene | 77 | 22 | 6.4 | 18 | 5.0 | 150 | 31 | 2.3 | 15 | 0.9 |
| Indeno[<i>cd</i>]pyrene | 61 | 14 | 17 | 14 | 14 | 150 | 39 | 23 | 33 | 20 |
| Dibenz[<i>a,h</i>]anthracene | 19 | 4.5 | 4.9 | 4.2 | 3.0 | 52 | 10 | 7.6 | n.d. | 5.3 |
| Benzo[<i>ghi</i>]perylene | 47 | 12 | 13 | 12 | 11 | 120 | 32 | 17 | 28 | 15 |
| Sum of PAHs | 2218 | 762 | 449 | 666 | 170 | 1759 | 604 | 235 | 427 | 139 |
| PAH decrease (%) | | 66 | 80 | 70 | 92 | | 66 | 87 | 76 | 92 |
| LMW/HMW ^a | 3.1 | 3.5 | 2.4 | 3.5 | 1.4 | 0.6 | 0.8 | 0.5 | 0.8 | 0.3 |
| 9-Fluorenone | 300 | 270 | 280 | 250 | 170 | 48 | 34 | 22 | 18 | 14 |
| Anthracene-9,10-dione | 72 | 50 | 60 | 45 | 40 | 33 | 17 | 11 | 11 | 7.9 |
| Benzo[<i>de</i>]anthracene- 7-one | 3.2 | 5.0 | n.d. | 5.0 | n.d. | 39 | 6.5 | 4.2 | 4.9 | n.d. |
| Benzo[<i>a</i>]anthracene- 7,12-dione | n.d. | 5.5 | 22 | 5.9 | 11 | 20 | 6.3 | 19 | 5.8 | 18 |
| Sum of O-PACs | 375 | 331 | 362 | 306 | 221 | 140 | 64 | 56 | 40 | 40 |
| O-PAC decrease (%) | | 12 | 3 | 18 | 41 | | 54 | 60 | 71 | 71 |
| %O-PAC (/total PAC) | 14 | 30 | 45 | 31 | 57 | 7 | 10 | 19 | 9 | 22 |

253 ^aLMW/HMW = ratio of sum of naphthalene to pyrene relative to sum of benzo[*a*]anthracene to benzo[*ghi*]perylene

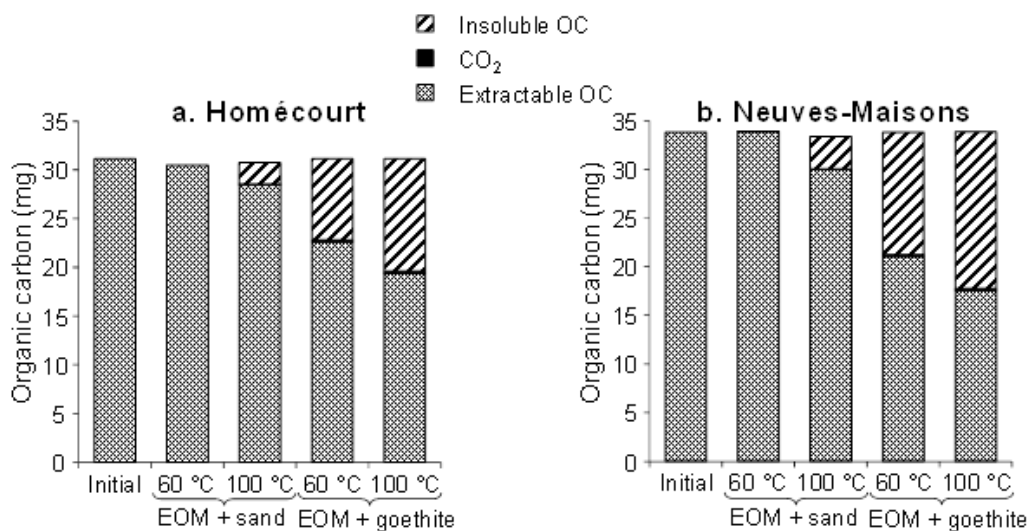
254 **4. Discussion**

255

256 4.1. Mechanisms of goethite-activated EOM oxidation

257 Overall, goethite showed a high reactivity during the EOM oxidation as CO₂ production and
258 the PAH degradation rate were enhanced by its presence. However, it should be noted that the
259 mineralization was of less importance because the amount of produced CO₂ during the
260 experiment remained very low (< 7% of TOC).

261 To give a better insight into the main process involved in the reduction of the PAH and EOM
262 contents, a carbon mass balance was performed (Figure 3). It showed that most of the carbon
263 from the initial EOM was transferred to the insoluble compartment. Such observations were
264 made in previous studies (Ghislain et al., 2010; Biache et al., 2011; Biache et al., 2014) where
265 air-oxidation of PAH associated with active minerals led to the decrease in EOM content and
266 to the formation of an insoluble carbonaceous residue resulting from oxidation-induced
267 polymerization.



268

269 *Figure 3: Carbon mass balance of the initial and oxidized samples of extractable organic matters*
270 *(EOMs) mixed with mineral phases (OC: organic carbon).*

271 EOM oxidations also induced an O-PAC production (ketones). Such compounds are known to
272 be produced during PAH oxidation in various contexts i.e. chemical oxidation (Lundstedt et
273 al., 2006), photo-degradation (Barbas et al., 1996) and biodegradation (Kazunga and Aitken,
274 2000). As the O-PAC production was much more important in the EOM/goethite mixture than
275 in the EOM/sand mixture, goethite seems to play an active part in the oxidation process. The
276 oxidation of organic compounds on goethite is known to be initiated by the sorption and then
277 formation of inner-sphere surface complexes with Fe^{III} surface sites (Pizzigallo et al., 1998).
278 This chemical coordination at the goethite surface is a prerequisite for the electron transfer
279 process (Stone and Morgan, 1987). Indeed, the sorbed molecule transfers an electron to Fe^{III}
280 site at goethite surfaces, leading to the formation of a very reactive cation radical that in turn
281 interacts with oxygen to produce oxygenated species (McBride, 1987). Finally, dissociation of
282 surface complexes and release of oxygenated species may occur, while the newly generated
283 Fe^{II} may be rapidly oxidized by O₂. Such mechanism was suggested for room temperature
284 oxidation of organic compounds by Mn^{VI}-Mn^{III}-oxides and Fe^{III}-oxides (McBride, 1987;
285 Stone and Morgan, 1987).

286 Our observations, i.e. important decrease in PAH contents and important production of O-
287 PACs, were consistent with the previously mentioned mechanism. This oxidation mechanism
288 must be favored by the increasing temperature, since more decay in EOM and PAH contents
289 and more O-PAC production were noted at 100 than at 60°C. Generally, the electron transfer
290 process induced by chemical complexation is considered as endothermic and therefore
291 improved by increasing temperature (Chidsey, 1991).

292 Moreover, several studies dealing with the Fe^{III}- or Mn^{III/IV}-induced oxidation of aromatic
293 compounds have pointed out same polymerization/condensation process as observed in this
294 study (Li et al., 2003; Arroyo et al., 2005; Russo et al., 2005).

295

296 4.2. Impact of goethite addition on the soil contamination.

297 When comparing the PAH decrease rates of both experiments (EOMs and soils), whole soils
298 seemed to be more reactive. Goethite addition had a different impact on the whole soil vs the
299 isolated EOM. While more decay in PAH concentration was observed in the presence of
300 goethite, less CO₂ was produced and O-PAC concentrations decreased. The EOM content did
301 not change significantly compared to the soil without goethite. The first explanation for these
302 differences is the presence in the soils of other –mineral and organic– reactive surfaces.
303 Previous studies dealing with biotic and abiotic oxidation of PAH contaminated matrices have
304 already pointed out a high reactivity of complex soil systems (Biache et al., 2011; Biache et
305 al., 2013; Biache et al., 2014) which has been attributed to the presence of reactive phases
306 such as clay minerals, metal oxides and organic macromolecules. Both soils contain such
307 reactive minerals (Biache et al., 2014), which may explain why the decrease in PAH and
308 EOM contents were already high in the soil without goethite addition. Similar mechanisms of
309 PAH oxidation could be involved here as in the EOM experiment but other by-products may
310 be formed. The decrease in O-PAC contents may be explained by a strong
311 sorption/sequestration in the soil and/or incorporation in the macromolecular network via
312 polymerization. The high decay of EOM in the whole soil compared to the EOM/mineral
313 mixture tends to support this hypothesis.

314 The goethite major impact was to reduce the CO₂ production in the whole soil experiment
315 even if the CO₂ amount remained very low in all investigated experiments (less than 7‰ and
316 4‰ of the Homécourt and Neuves-Maisons soils, respectively). This slight discrepancy “soil
317 vs soil/goethite” might be due to CO₂ adsorption on goethite surfaces, but this process cannot
318 be quantitatively evaluated in soil complex systems (Russell et al., 1975).

319

320 4.3. Impact of initial soil composition on the OM reactivity

321 While both EOMs exhibited similar global trends during oxidations, some molecular-level
322 differences can be observed. For example during the mineral/EOM oxidation, O-PAC
323 compounds were produced for both EOMs; however the distribution of the generated
324 compounds was different (Table 1, Figures S5 and S6). Indeed, the main O-PACs produced
325 during Homécourt EOM oxidation were 3-ring O-PACs (9-fluorenone and anthracene-9,10-
326 dione) whereas for Neuves-Maisons EOM oxidation, 4-ring O-PACs (benzo[*de*]anthracene-7-
327 one and benz[*a*]anthracene-7,12-dione) were predominantly generated. These discrepancies
328 can be attributed to differences in the initial PAH soil composition; Homécourt sample being
329 dominated by 3-ring PAHs (Table 1, Figure S3) and Neuves-Maisons being dominated by 4-
330 and 5-ring PAHs (Table 1, Figure S4). It is worthwhile noting that PAHs are known to be
331 precursors of O-PAC formation. For instance 9-fluorenone is known to be one of the
332 oxidation product of fluorene (Lee et al., 2001) which occurs in high concentration in
333 Homécourt sample and, similarly, benz[*a*]anthracene-7,12-dione can be generated during
334 benz[*a*]anthracene oxidation (Lee et al., 2001) which is one of the major PAHs of Neuves-
335 Maisons sample.

336 Difference of the initial sample composition also seems to influence the sample response to
337 oxidation. For both EOM/mineral and soil oxidations, the decrease in EOM contents was
338 more important for Neuves-Maisons samples than for Homécourt (Figure 2). As discussed,
339 this decrease was a transfer of the organic carbon from the EOM to the insoluble fraction
340 which was more important for Neuves-Maisons than for Homécourt (Figure 3). The latter
341 observation can be due to the fact that Neuves-Maisons sample presented higher proportion of

342 HMW compounds than Homécourt and HMW compounds are more inclined to be stabilized
343 (condensed) in the non-extractable fraction (Northcott and Jones, 2001).

344

345 **5. Summary and conclusion**

346 In all experiments, oxidation led to (i) a decrease in PAH concentrations, (ii) a low production
347 of CO₂ and (iii) a decrease in EOM content due to a condensation/polymerization
348 phenomenon evidenced by a carbon mass balance. Oxidation of the EOM/minerals also led to
349 a production of O-PACs, the initial PAH soil composition governing the type of generated
350 compounds. The oxidation effects were more pronounced for EOM/goethite mixture than for
351 EOM/silica sand mixture. These observations are consistent with the famous goethite-induced
352 transformation mechanism of organic compounds. After PAC sorption on goethite surfaces,
353 electron transfer process occurs leading to the formation of reactive cation radical that in turn
354 interacts with oxygen or oxygen-species yielding oxidized products.

355 As in EOM experiments, goethite addition to the whole soils affected OM oxidation, but in a
356 lesser extent. This limited effect was likely due to the presence of a significant amount of
357 reactive phases naturally occurring in the soils. The soil initial composition also impacted its
358 evolution during oxidation; higher abundance of HMW compounds favoring the formation of
359 an insoluble residue and therefore EOM stabilization.

360 These conclusions showed that goethite may play a part in natural attenuation of PAH
361 contaminated soils as it contributes to contamination stabilization during low-temperature air-
362 oxidation. This work provides first results of the mechanisms involved and also underlined
363 the potential of indigenous reactive minerals to stabilize organic contamination. Therefore
364 their impact on the fate and transformation of PAHs in soils under different conditions
365 (humidity, temperature, oxygen concentrations) more representative of the field should be

366 investigated , and the long-term behavior of the refractory compounds generated during
367 oxidation (e.g. insoluble carbonaceous residues) should be explored.

368

369 **Acknowledgements**

370 We thank the GISFI (French Scientific Interest Group - Industrial Wasteland
371 (<http://www.gisfi.prd.fr>). We thank Pr. Christian Ruby from the LCPME laboratory (Nancy)
372 for supplying us with the goethite.

373

374 **References**

- 375 Arroyo, L.J., Li, H., Teppen, B.J., Johnston, C.T., Boyd, S.A., 2005. Oxidation of 1-naphthol
376 coupled to reduction of structural Fe³⁺ in smectite. *Clays Clay Miner.* 53, 587-596.
- 377 Barbas, J.T., Sigman, M.E., Dabestani, R., 1996. Photochemical oxidation of phenanthrene
378 sorbed on silica gel. *Environ. Sci. Technol.* 30, 1776-1780.
- 379 Biache, C., Faure, P., Mansuy-Huault, L., Cébron, A., Beguiristain, T., Leyval, C., 2013.
380 Biodegradation of the organic matter in a coking plant soil and its main constituents.
381 *Org. Geochem.* 56, 10-18.
- 382 Biache, C., Ghislain, T., Faure, P., Mansuy-Huault, L., 2011. Low temperature oxidation of a
383 coking plant soil organic matter and its major constituents: An experimental approach to
384 simulate a long term evolution. *J. Hazard. Mater.* 188, 221-230.
- 385 Biache, C., Kouadio, O., Lorgeoux, C., Faure, P., 2014. Impact of clay mineral on air
386 oxidation of PAH-contaminated soils. *Environ Sci Pollut Res*, 1-10.
- 387 Blanchart, P., Faure, P., Bruggeman, C., De Craen, M., Michels, R., 2012. In situ and
388 laboratory investigation of the alteration of Boom Clay (Oligocene) at the air–

389 geological barrier interface within the Mol underground facility (Belgium):
390 Consequences on kerogen and bitumen compositions. *Appl. Geochem.* 27, 2476-2485.

391 Borch, T., Kretzschmar, R., Kappler, A., Cappellen, P.V., Ginder-Vogel, M., Voegelin, A.,
392 Campbell, K., 2009. Biogeochemical redox processes and their impact on contaminant
393 dynamics. *Environ. Sci. Technol.* 44, 15-23.

394 Calemma, V., Rausa, R., Margarit, R., Girardi, E., 1988. FT-i.r. study of coal oxidation at low
395 temperature. *Fuel* 67, 764-770.

396 Chidsey, C.E.D., 1991. Free energy and temperature dependence of electron transfer at the
397 metal-electrolyte Interface. *Science* 251, 919-922.

398 Elie, M., Faure, P., Michels, R., Landais, P., Griffault, L., 2000. Natural and laboratory
399 oxidation of low-organic-carbon-content sediments: comparison of chemical changes in
400 hydrocarbons. *Energy Fuels* 14, 854-861.

401 Faure, P., Landais, P., Griffault, L., 1999. Behavior of organic matter from Callovian shales
402 during low-temperature air oxidation. *Fuel* 78, 1515-1525.

403 Gethner, J.S., 1987. Kinetic study of the oxidation of Illinois No. 6 coal at low temperatures:
404 Evidence for simultaneous reactions. *Fuel* 66, 1091-1096.

405 Ghislain, T., Faure, P., Biache, C., Michels, R., 2010. Low-temperature, mineral-catalyzed air
406 oxidation: a possible new pathway for PAH stabilization in sediments and soils.
407 *Environ. Sci. Technol.* 44, 8547-8552.

408 Jakab, E., Hoesterey, B., Windig, W., Hill, G.R., Meuzelaar, H.L.C., 1988. Effects of low
409 temperature air oxidation (weathering) reactions on the pyrolysis mass spectra of US
410 coals. *Fuel* 67, 73-79.

411 Kazunga, C., Aitken, M.D., 2000. Products from the incomplete metabolism of pyrene by
412 polycyclic aromatic hydrocarbon-degrading bacteria. *Appl. Environ. Microbiol.* 66,
413 1917-1922.

414 Lee, B.-D., Iso, M., Hosomi, M., 2001. Prediction of Fenton oxidation positions in polycyclic
415 aromatic hydrocarbons by Frontier electron density. *Chemosphere* 42, 431-435.

416 Li, H., Lee, L.S., Schulze, D.G., Guest, C.A., 2003. Role of soil manganese in the oxidation
417 of aromatic amines. *Environ. Sci. Technol.* 37, 2686-2693.

418 Lin, K., Ding, J., Wang, H., Huang, X., Gan, J., 2012. Goethite-mediated transformation of
419 bisphenol A. *Chemosphere* 89, 789-795.

420 Lundstedt, S., Persson, Y., Öberg, L., 2006. Transformation of PAHs during ethanol-Fenton
421 treatment of an aged gasworks' soil. *Chemosphere* 65, 1288-1294.

422 McBride, M.B., 1987. Adsorption and oxidation of phenolic compounds by iron and
423 manganese oxides. *Soil Sci. Soc. Am. J.* 51, 1466-1472.

424 Nam, K., Rodriguez, W., Kukor, J.J., 2001. Enhanced degradation of polycyclic aromatic
425 hydrocarbons by biodegradation combined with a modified Fenton reaction.
426 *Chemosphere* 45, 11-20.

427 Northcott, G.L., Jones, K.C., 2001. Partitioning, extractability, and formation of
428 nonextractable PAH residues in soil. 1. Compound Differences in Aging and
429 Sequestration. *Environ. Sci. Technol.* 35, 1103-1110.

430 Pizzigallo, M.D.R., Ruggiero, P., Crecchio, C., Mascolo, G., 1998. Oxidation of
431 chloroanilines at metal oxide surfaces. *J. Agr. Food Chem.* 46, 2049-2054.

432 Prélot, B., Villiéras, F., Pelletier, M., Gérard, G., Gaboriaud, F., Ehrhardt, J.-J., Perrone, J.,
433 Fedoroff, M., Jeanjean, J., Lefèvre, G., Mazerolles, L., Pastol, J.-L., Rouchaud, J.-C.,
434 Lindecker, C., 2003. Morphology and surface heterogeneities in synthetic goethites. *J.*
435 *Colloid Interface Sci.* 261, 244-254.

436 Russell, J.D., Paterson, E., Fraser, A.R., Farmer, V.C., 1975. Adsorption of carbon dioxide on
437 goethite (α -FeOOH) surfaces, and its implications for anion adsorption. *J. Chem. Soc.,*
438 *Faraday Trans.* 71, 1623-1630.

439 Russo, F., Rao, M., Gianfreda, L., 2005. Bioavailability of phenanthrene in the presence of
440 birnessite-mediated catechol polymers. *Appl. Microbiol. Biotechnol.* 68, 131-139.

441 Schwertmann, U., Cornell, R.M., 2007. Goethite. in *Iron oxides in the laboratory* 2nd Ed.
442 Wiley-VCH Verlag GmbH, pp. 67-92.

443 Schwertmann, U., Taylor, R.M., 1989. Iron Oxides. in: Dixon, J.B., Weed, S.B. (Eds.).
444 Minerals in soil environments. Soil Science Society of America, pp. 379-438.

445 Stone, A.T., Morgan, J.J., 1987. Reductive dissolution of metal oxides. in: *Aquatic surface*
446 *chemistry: chemical processes at the particle-water interface.* John Wiley and Sons,
447 New York. 1987. p 221-254.

448 Sumner, M.E. (Ed.), 2000. *Handbook of soil science.* CRC Press LLC.

449 Usman, M., Faure, P., Lorgeoux, C., Ruby, C., Hanna, K., 2013. Treatment of hydrocarbon
450 contamination under flow through conditions by using magnetite catalyzed chemical
451 oxidation. *Environ Sci Pollut Res* 20, 22-30.

452 Usman, M., Faure, P., Ruby, C., Hanna, K., 2012. Remediation of PAH-contaminated soils by
453 magnetite catalyzed Fenton-like oxidation. *Appl. Catal., B* 117–118, 10-17.

454 Wang, Y., Liu, C.S., Li, F.B., Liu, C.P., Liang, J.B., 2009. Photodegradation of polycyclic
455 aromatic hydrocarbon pyrene by iron oxide in solid phase. *J. Hazard. Mater.* 162, 716-
456 723.

457 Watts, R.J., Stanton, P.C., 1999. Mineralization of sorbed and NAPL-phase hexadecane by
458 catalyzed hydrogen peroxide. *Water Res.* 33, 1405-1414.

459 Yap, C.L., Gan, S., Ng, H.K., 2011. Fenton based remediation of polycyclic aromatic
460 hydrocarbons-contaminated soils. *Chemosphere* 83, 1414-1430.

461 Zhang, H., Huang, C.-H., 2007. Adsorption and oxidation of fluoroquinolone antibacterial
462 agents and structurally related amines with goethite. *Chemosphere* 66, 1502-1512.